JACS
JOURNAL OF THE AMERICAN CHEMICAL SOCIETY

ARTICLE

pubs.acs.org/JACS

Genetic Analysis of H1N1 Influenza Virus from Throat Swab Samples in a Microfluidic System for Point-of-Care Diagnostics

B. Scott Ferguson,[†] Steven F. Buchsbaum,[‡] Ting-Ting Wu,[§] Kuangwen Hsieh,[†] Yi Xiao,[†,∥] Ren Sun,[§] and H. Tom Soh*[,†,∥,§]

[†]Department of Mechanical Engineering, [∥]Materials Department, and [‡]College of Creative Studies, University of California, Santa Barbara, Santa Barbara, California 93106, United States

[§]Department of Molecular and Medical Pharmacology, University of California, Los Angeles, Los Angeles, California 90095, United States

Supporting Information

ABSTRACT: The ability to obtain sequence-specific genetic information about rare target organisms directly from complex biological samples at the point-of-care would transform many areas of biotechnology. Microfluidics technology offers compelling tools for integrating multiple biochemical processes in a single device, but despite significant progress, only limited examples have shown specific, genetic analysis of clinical samples within the context of a fully integrated, portable platform. Herein we present the Magnetic Integrated Microfluidic Electrochemical Detector (MIMED) that integrates sample preparation and electrochemical sensors in a monolithic disposable device to detect RNA-based virus directly from throat swab samples. By combining immunomagnetic target capture, concentration, and purification, reverse-transcriptase polymerase chain reaction (RT-PCR) and single-stranded DNA (ssDNA) generation in the sample preparation chamber, as well as sequence-specific electrochemical DNA detection in the electrochemical cell, we demonstrate the detection of influenza H1N1 in throat swab samples at loads as low as 10 $TCID_{50}$, 4 orders of magnitude below the clinical titer for this virus. Given the availability of affinity reagents for a broad range of pathogens, our system offers a general approach for multitarget diagnostics at the point-of-care.

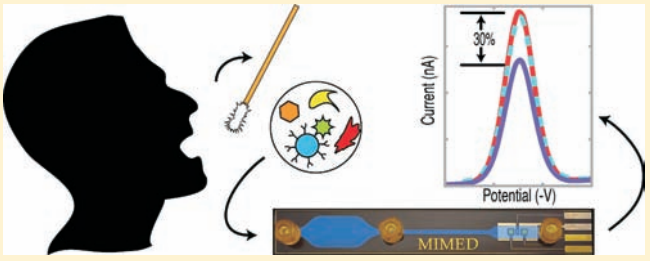

INTRODUCTION

There exists a general need for technologies that enable sensitive, accurate, and sequence-specific genetic detection of rare target organisms (e.g., viruses, bacteria, or mammalian cells) within complex biological samples for a broad variety of biotechnology applications, including forensics,[1] food safety,[2] environmental monitoring,[3] and clinical diagnostics[4−7] at the point-of-care (POC). Specifically, due to the low titers of target organisms and the complexity of clinical samples, direct detection is met with severe technical challenges.[8] For example, influenza tests from untreated throat and nasopharyngeal swabs typically contain sample-degrading nucleases, PCR inhibitors, and aggregating factors.[9−12] For *E. coli* O157:H7 stool sample tests, pathogen levels typically fall below $\sim 10^5$ colony-forming units per milliliter (CFU mL^{-1}) and exist in a mixture of a background of nonpathogenic strains, PCR inhibitors, and cellular debris.[13−15]

Thus, it is apparent that effective sample preparation, including concentration and purification of target species from complex backgrounds, holds the key for direct molecular detection at the POC. Furthermore, in order to minimize sample loss and achieve rapid detection, it is imperative to integrate sample preparation with the detection assay in a single device. Toward this end, a number of groups have explored the use of microfluidics technology as a means for integrating sample preparation, genetic amplification, and molecular readout.[16−18] However, this goal has proven to be technically challenging to achieve, and only a few limited examples have reported the sequence-specific genetic analysis of target species at relevant concentrations, directly from unprocessed patient samples.[19−21] Achieving this goal is especially important for electrochemical-based platforms, which are well suited for POC applications due to their portability, robustness, and integration with circuitry.[22−25]

Toward a universal solution for electrochemical sequence-specific genetic detection at the point-of-care, we present here the Magnetic Integrated Microfluidic Electrochemical Detector (MIMED) (Figure 1). This system integrates high-throughput immunomagnetic target capture, concentration, and purification, efficient on-chip reverse-transcriptase polymerase chain reaction (RT-PCR), single-stranded DNA (ssDNA) generation, and sequence-specific electrochemical detection, all in an integrated, monolithic device. By taking advantage of the multifuncational sample preparation chamber which enables high-throughput

Received: April 29, 2011
Published: May 11, 2011

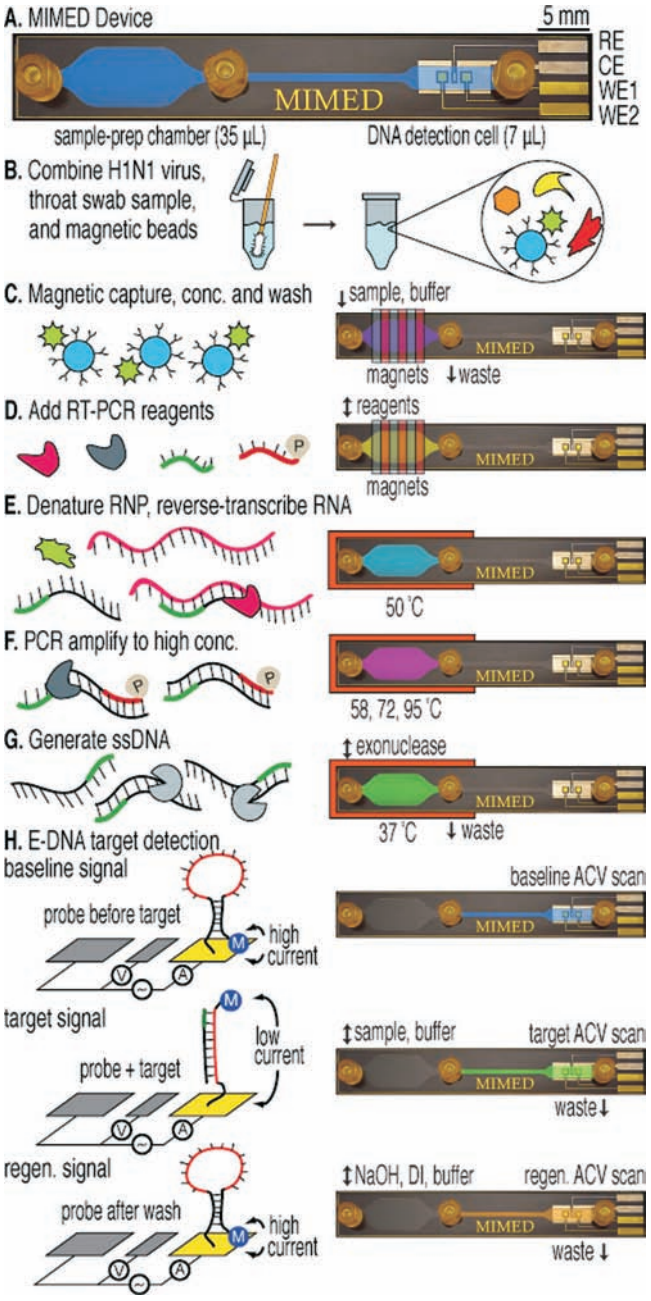

Figure 1. Sample-to-answer genetic analysis of H1N1 virus. (A) The 1 × 6 cm device features three fluidic ports: sample/buffer/reagent input (left), waste output (center), and E-DNA product output (right). Capture, RT-PCR, and ssDNA generation are performed in the sample preparation chamber; detection is performed in the electrochemical DNA detection cell. (B) A throat swab is collected and combined with influenza virus and antibody-coated magnetic beads in a tube containing RNA stabilizer. (C) The sample is pumped into the device where external magnets capture, concentrate, and purify labeled viral RNP in the sample preparation chamber. (D) RT-PCR mix is injected. (E) The chip is heated to denature the RNP and release the RNA. (F, G) RT-PCR is performed on-chip followed by lambda exonuclease-mediated ssDNA generation. (H) Product is pumped into the DNA detection cell, where hybridization is measured via AC voltammetry.

target enrichment, the prevention of nonspecific enzyme adsorption, high PCR efficiency, and lossless integration with the target-specifc signaling probe, this system can be configured to detect a wide range of RNA- or DNA-based pathogens in unprocessed samples. As a model, we demonstrate the specific, genetic detection of H1N1 viruses directly from throat swabs within 3.5 h and a limit of detection (LOD) of 10 $TCID_{50}$, approximately 4 orders of magnitude below the clinically relevant infectious dose.

EXPERIMENTAL SECTION

Quantifying Viral Enrichment from Swab Samples. To compare the effects of sample preparation, each experiment was replicated in triplicate in three separate one-time-use devices. Positive controls were prepared by adding 1 μL of antibody-coated beads (10^6) and 1 μL of viral particles (10^4 $TCID_{50}$) to 50 μL of standard RT-PCR mixture plus 1X SYBR green. 'Direct detection' samples were prepared likewise, with a throat swab first added to the mix for 5 min. The MIMED 'complete prep' samples were conducted by adding a throat swab to 1 mL of 10% RNAlater solution for 5 min followed by addition of 1 μL of antibody-coated beads and 1 μL of viral particles. This solution was incubated for 30 min at 4 °C and then pumped through the device at 60 mL h^{-1} with permanent magnets applied, followed by a 1 mL wash with PBS at the same flow rate. The magnets were then removed, and the beads were eluted with 50 μL of RT-PCR mixture. 'Magnetic particle concentrator' (MPC) samples were processed with 5 min of magnetic capture time in place of the above flow rates. 'No concentration' samples were prepared like the 'complete prep' samples but by stopping sample flow after the trapping chamber became full to prevent concentration. 'No RNA stabilization' samples were prepared with initial incubation in PBS rather than 10% RNAlater. 'No wash' samples were prepared with RT-PCR mix elution immediately following capture, thereby excluding the wash step. Additionally, in order to isolate the effects of eliminating washing without the PCR inhibitory effects of residual RNAlater or the degradation effects arising from absence of RNAlater, viral particles were added after completion of the 'no wash' MIMED sample preparation. Negative controls were prepared like that for the MIMED samples but without adding viral particles. Quantitative RT-PCR was run with the same parameters as in the MIMED assay but with 55 cycles to enable recalcitrant samples to cross the threshold level.

Viral Sample Preparation. Influenza A/PR/8/34 H1N1 was propagated on MDCK (Madin−Darby canine kidney) cells and virus-containing supernatants were harvested when 80% of cells showed cytopathic effects. The supernatants were clarified twice by centrifugation at 4 °C and then stored in aliquots at −80 °C. Viral titers were determined by measuring $TCID_{50}$ using MDCK cells.[26] The influenza viral RNA exists in a native complex with the viral nucleoprotein, known as the ribonucleoprotein (RNP). We exploit this RNP for high-efficiency target RNA capture via the anti-influenza A nucleoprotein antibody. The lipid envelope of the harvested virus is disrupted to release the intact RNP by diluting virus-containing supernatant (10^8 $TCID_{50}$ mL^{-1}) 10-fold in buffer containing 50 mM Tris-HCl (pH 7.5), 150 mM NaCl, 1 mM EDTA, and 2% NP-40 (Sigma Aldrich, St. Louis, MO).[27] This step allows for safe handling and improves the access of the antibody to the target nucleoprotein, thereby increasing the efficiency of the target RNA capture. The mixture was incubated at 4 °C for 1 h and then stored at −80 °C in aliquots.

Viral RNP Capture. We thawed the stock virus and diluted it to the desired concentration with 1X PBS. One microliter of this dilution was added to capture buffer, followed by 5 μL (~10^7) of streptavidin-coated magnetic beads (diameter = 1 μm) conjugated with biotinylated anti-influenza A nucleoprotein. Samples were rotated for 30 min at 4 °C. For initial MIMED system tests, 1 mL of 1X PBS was used as capture buffer, while the simulated patient samples used 10% RNAlater (Qiagen, Valencia, CA) in 1X PBS as the capture buffer to mitigate RNA degradation. Throat swabs were collected from a healthy donor with

flocked nylon swabs (VWR LabShop, Batavia, IL) and incubated in 50 μL of capture buffer for 5 min prior to the addition of virus and beads. After incubation, the device chamber was placed above six permanent NeFeB magnets (K&J Magnetics, Inc., Jamison, PA) while the sample solution was pumped through the chip at 60 mL h^{-1} via a syringe pump (Next Advance Inc., Averill Park, NY). The trapped beads were then washed by flowing 1 mL of 1X PBS through the chamber at 60 mL h^{-1} to remove interferents. Magnetic separation is effective for a wide range of biological targets,[28,29] and this approach has proven particularly advantageous for achieving high-throughput capture with minimal loss within the context of a microfluidic channel.[30−33]

Magnetic Trapping Simulations. In the sample preparation chamber, the Reynolds number (Re) was calculated to be ∼1 at a flow rate (Q) of 60 mL h^{-1}. Thus, the magnetic beads would experience a Stokes drag force of $F_d = 6\pi\eta a(v_f - v_p)$, where a is the bead diameter, and v_f and v_p are the velocities of the fluid and particle, respectively. When a strong magnetic field (B) is applied via external neodymium iron boron (NeFeB) permanent magnets, the magnetic force exerted on the bead is taken as $F_m = (4/3)\pi r^3 \rho M \nabla B$, where r is the radius, ρ is the density, and M is the saturation magnetization of the bead (∼23.5 Am^2 kg^{-1}).[34] The governing equations of magnetostatics and incompressible flow were solved to yield the magnetic force and velocity fields. By balancing the magnetic and drag forces on a given bead, the transport equations were solved, yielding the bead concentration profile through the channel. The minimum bead residence time necessary for 100% capture was expressed as the time required for a bead to translate to the capture plane from the opposing channel. The drag on an immobilized bead was estimated as the Stokes drag force with a velocity differential equal to the flow speed one bead radius away from the channel surface.

To test the agreement between simulations of capture efficiency and experimental results, we pumped suspensions of phycoerythrin-labeled beads in 1X PBS (10^7 beads mL^{-1}) through the chip at 6.0, 60, or 600 mL h^{-1}, followed by washing at the same flow-rate, to measure bead retention. The beads eluted at the outlet with or without magnets were measured in triplicate by flow cytometry (BD FACSAria, NJ). Capture efficiency was calculated based on the number of beads trapped as normalized against the counts from the nonmagnetized control. This does not include beads that may have been lost in the interfacing common to both groups; however, such loss was measured as <2%.

RT-PCR and ssDNA Generation. We injected 50 μL of RT-PCR mix (OneStep RT-PCR kit, Qiagen, Valencia, CA) containing RT-PCR buffer (10 μL, 5X initial), a phosphorylated forward primer and standard reverse primer (3 μL each, 10 μM initial), dNTP (2 μL, 10 mM initial), enzyme (2 μL, 25X initial), and deionized water (remaining volume) into the chamber over the trapped virus. The chip was mounted onto a thermoelectric cooler (TEC, Custom Thermoelectric, Bishopville, MD) linked to a PID controller (Omega Engineering, Inc., Stamford, CT), which was heated to 50 °C for 30 min to denature protein−RNA complexes. The sample was then subjected to a 15 min hot start at 95 °C followed by 38 cycles of 95 °C, 55 °C, and 72 °C with 30 s dwells and average ramp rate of ∼1 °C s^{-1}. Following amplification, ssDNA was generated. The PCR product solution was mixed 10:1 with 10X lambda exonuclease enzyme stock (New England Biolabs, Ipswich, MA) and incubated in the reaction chamber for 20 min at 37 °C directly with no purification steps. The ssDNA generation efficiency was measured by fluorescence (Gel Logic EDAS 200, Kodak, Rochester, NY). Fluid transport was conducted either manually via syringes or via automated syringe pump (PhD 2000, Harvard Apparatus, Holliston, MA). Mixing was facilitated by introducing reagents into the device in preloaded syringes and pumping back and forth. Additional fluid volume exceeding the device chamber capacity was simply retained in the syringe. Exploiting the syringes as mixing chambers exhibited efficiency indistinguishable from traditional pipet-aided mixing in a tube, and negated the need for on-chip mixers, thereby significantly decreasing the complexity and cost of the disposable chip, increasing the value at the POC.

On-Chip E-DNA Measurements. The working electrodes of the electrochemical detection cell feature DNA oligonucleotide probes complementary to the 20-base-pair region in segment 7 of influenza A/PR/8/34/H1N1, which have been immobilized via gold−thiol chemistry. All voltammetric scans were conducted in the E-DNA cell in the presence of 1X high-salt incubation E-DNA buffer (HSIEB, 1.5 M NaCl, 100 mM phosphate, 1 mM Mg^{2+}) to maintain consistent salt concentration and pH. To establish baseline signals, the DNA detection cell was flushed with 1X HSIEB and alternating current voltammetry (ACV) scans were taken prior to sample injection. Subsequently, the PCR product was drawn into a syringe containing an equal volume of 2X HSIEB, mixed, and injected into the DNA detection cell for hybridization with probes for 30 min at room temperature after which ACV signals were measured. Finally, the E-DNA probes were regenerated by pumping 1 mL of 50 mM NaOH followed by 5 mL of deionized water through the cell, and the sensor was scanned again in the presence of 1X HSIEB. ACV was performed between −0.7 V and −0.2 V, at a frequency of 100 Hz, an amplitude of 10 mV and sensitivity of 500 nA.

RESULTS AND DISCUSSION

MIMED System Overview. The entire influenza H1N1 detection was performed within a single MIMED device from throat swab samples. The MIMED device is microfabricated with PDMS and glass materials and contains two physical modules: the sample preparation chamber (35 μL) and electrochemical DNA detection cell (7 μL) (Figure 1A). Briefly, the target capture, concentration and purification, RT-PCR amplification, and ssDNA generation are performed within the sample preparation chamber. This chamber is designed for (1) high-throughput magnetic capture enabled by reduced drag and large magnetic field gradients, (2) the prevention of nonspecific enzyme adsorption by the incorporation of low PDMS surface area[35,36] without ferromagnetic structures,[37,33] and (3) high PCR efficiency enabled by uniform heating across the low-aspect ratio channel. The amplicon detection is achieved by the E-DNA probes in the DNA detection cell. The E-DNA probes undergo a specific target binding-induced conformation change,[37,38] and the detection cell is designed for seamless integration with the sample preparation chamber without the need for intermediate purification steps. The cell contains platinum counter (CE) and reference (RE) electrodes, and two gold working electrodes (WE) for duplicate measurement of the E-DNA probe signal. The details of the device and probe fabrication are provided in the Supporting Information (Figure S1).

MIMED-Based H1N1 Virus Genetic Analysis. To mimic a clinical sample of known viral load, each swab was obtained from a healthy donor and combined with the desired viral titer in a vial of RNA stabilization medium with antibody-coated magnetic beads. Influenza RNA exists in a stable complex with the nucleoprotein, known as the ribonucleoprotein (RNP). Thus, to capture the target RNA, we capture the RNP complex via an antinucleoprotein antibody (Figure 1B). After the bead/sample incubation, the sample is injected into the MIMED sample preparation chamber where magnetic forces capture and concentrate the magnetically labeled target. During trapping, we remove interferents from the swab sample by continuous washing in the microchamber (Figure 1C). Next we inject RT-PCR mix containing a phosphorylated primer into the chamber (Figure 1D). The RNP complex is thermally denatured to enable

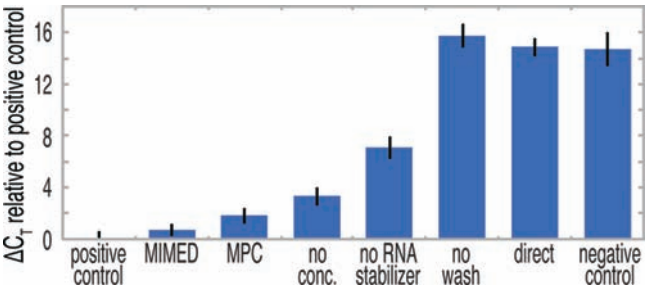

Figure 2. Enrichment of nucleic acids from swab samples as measured by the change in PCR threshold cycles. ΔC_T values were determined with respect to the positive control, which consisted of viral particles spiked directly into PCR mix without swab-based interferents. MIMED sample enrichment, consisting of concentration, RNA stabilization, and continuous washing, approached the positive control (ΔC_T = 0.7), indicating efficient capture and purification of nucleic acids. Performing these steps in a magnetic particle concentrator (MPC) resulted in moderate sample loss (ΔC_T = 1.8). Excluding any one MIMED preparation step incurred significant enrichment penalties. Forgoing all three steps yields results equivalent to that of the zero-virus negative control.

reverse transcription of the captured RNA target (Figure 1E). The newly obtained cDNA target is then PCR amplified to yield up to a ~300 nM amplicon concentration within the microchamber (Figure 1F). We selectively digest the phosphorylated strands[40] from the dsDNA amplicons with lambda exonuclease[41] to obtain ssDNA necessary for subsequent sequence-specific detection (Figure 1G). Finally, this ssDNA product is mixed with high-salt buffer and delivered to the DNA detection cell to hybridize with a redox-labeled, electrode-bound E-DNA signaling probe (Figure 1H). Target hybridization induces a conformational change in the E-DNA probe, forcing the redox label away from the WE, decreasing faradic current. The relative current change due to the amplified target DNA corresponds to the initial viral quantity in the samples. To verify that the signal was the result of target hybridization, we flushed dehybridization buffer through the cell, removing the target and regenerating the sensor.

Viral RNA Capture, Concentration and Purification from Swab Samples. Clinical samples usually contain a low concentration of target among a high concentration of background including target-degrading components and interferents, which inhibit downstream enzymatic processes.[9−12] Thus, rare target detection from unprocessed patient samples at the POC requires efficient sample preparation, which we achieved through a combination of viral RNP concentration, RNA stabilization, and removal of interferents. In the clinical setting, swab samples are typically eluted directly into a vial of transport medium. In our assay, we replaced the transport medium with a solution containing (1) nonionic detergent to dissolve the viral envelope and release intact RNP-containing target RNA,[27] (2) RNA stabilizer to protect this target RNA from degradation, and (3) antibody-coated magnetic beads to capture the released and protected RNP. The sample is injected into the device, and high-gradient magnetic capture was used to concentrate the viral RNA on-chip, obviating the need for time-consuming benchtop procedures such as phenol−chloroform extraction.[42] PCR inhibitors present in the swab sample were then removed via a continuous washing with buffer within the device.

The MIMED system shows remarkable RNA enrichment from swab samples (Figure 2); for example, the MIMED sample

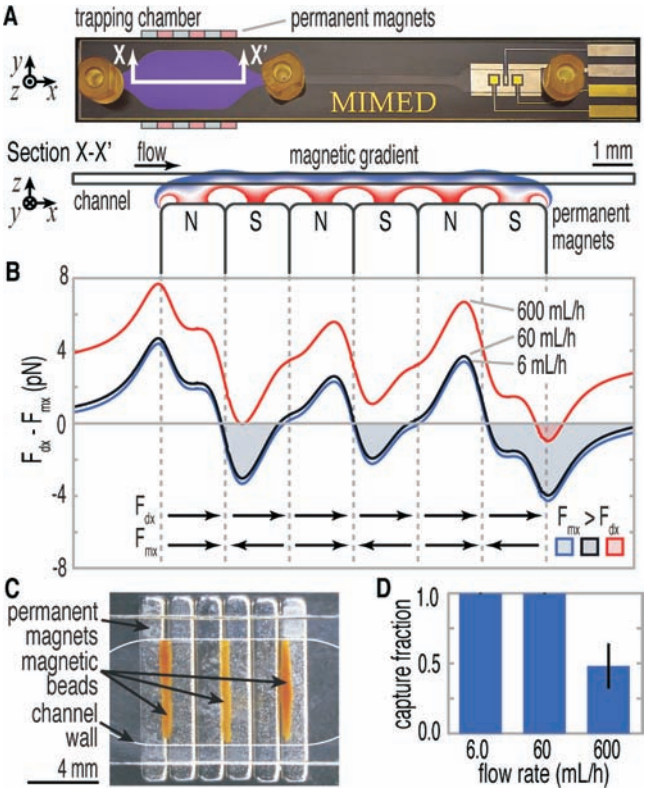

Figure 3. Simulation of magnetic capture. (A) Section view of the MIMED trapping chamber illustrates the magnetic gradient across the channel wherein beads experience a pull-down force of ~10 pN. (B) Sum of the magnetic (F_{mx}) and drag forces (F_{dx}) exerted on a stationary bead at 6, 60, 600 mL h^{-1}. At 6 and 60 mL h^{-1}, F_m exceeds F_d throughout all three trapping regions, enabling efficient bead capture (shaded regions). However, at 600 mL h^{-1}, this only occurs by a narrow margin in the last trapping region (<1 pN), suggesting potential for sample loss. (C) Experimental verification of simulation predictions of bead capture at the three stable equilibria established by the permanent magnets. (D) Efficiency of bead capture is measured vs flow rate. Triplicate trials indicated ~100 ± 0.3% bead capture at 6.0 and 60 mL h^{-1}. At 600 mL h^{-1}, capture efficiency decreases to ~48 ± 16%.

preparation performance nearly matches the ideal lossless positive control (an equal quantity of purified viral particles doped directly into PCR mix), with ΔC_T = 0.7. We use ΔC_T (defined as the difference in threshold cycle value between a given sample and the positive control) to quantify the signals, as it directly relates the difference in nucleic acid template copy number between samples.[43] PCR efficiency was determined from the standard curve to be ε = 1.94, indicating efficient amplification compared to the theoretical maximum of ε = 2, and corresponding to 10-fold difference in template copy number for each ΔC_T = 3.48. As a comparison, the same sample preparation procedure performed in a magnetic particle concentrator (MPC, Invitrogen) enriched less effectively (ΔC_T = 1.8) possibly due to inferior washing or bead loss. Dramatic signal loss was evident upon omission of any of the three MIMED sample preparation steps. For example, the absence of RNA concentration or stabilization resulted in ΔC_T penalties of 3.3 and 7.1, respectively, the latter indicating that RNA targets were significantly degraded by nucleases and aggregating factors present in the swab samples.[10,44−46] Excluding the washing step resulted in ΔC_T = 15.8, rendering the samples to be indistinguishable from

the zero-virus negative control (ΔC_T = 14.7), potentially due to degrading factors and PCR inhibitors. The omission of all three steps, directly spiking virus-treated swab samples into PCR mix, yielded a ΔC_T of 14.9, indicating the absence of a positive signal from target RNA due to background interferents. These results clearly illustrate that each element in MIMED sample preparation is necessary.

Characterization of Integrated Magnetic Capture. The high-throughput, low-loss, immunomagnetic sample purification within the MIMED device is achieved by ensuring that the magnetophoretic force (F_m) is sufficient to (1) efficiently attract immunomagnetically labeled viruses to the trapping surface from any point in the flow stream and (2) exceed the fluidic drag (F_d) for sustained retention during washing.[30,47] Using finite element simulation (COMSOL Multiphysics, Stockholm, Sweden), we calculated that the magnetic field gradient (∇B) in the vertical direction is >300 T m^{-1} across the chamber, exerting a force of ~10 pN on the magnetic beads (Supporting Information, Figure S2A).[34] By balancing magnetophoretic and fluidic drag forces in the vertical direction, we determined that a ~1 s residence time is necessary to attract all magnetic beads in solution to the trapping surface. Because of the wide-channel geometry, our device is capable of operating at a volume throughput up to 600 mL h^{-1} (Figure S2B). Next, we investigated the retention of beads during the washing procedure by calculating the sum of the forces in the x-direction ($F_{dx} + F_{mx}$) experienced by the magnetically labeled virus captured on the trapping surface, as shown in Figure 3B. In order for trapping to occur, the magnetic force must exceed the maximum drag force ($F_{mx} > F_{dx}$). F_{dx} on a captured bead is directly proportional to the fluid velocity and is expected to exceed F_{mx} at high flow rates, resulting in bead losses. We experimentally confirmed that capture occurs at the left of the trapping regions, where the F_{mx} field converges and equilibrates with F_{dx} (Figure 3C). Consistent with our simulation, approximately 100 ± 0.3% of the beads were captured at flow rates of 6.0 and 60 mL h^{-1} (Figure 3D). At 600 mL h^{-1}, the capture efficiency decreased to 48 ± 16%. Thus, we selected 60 mL h^{-1} as the nominal flow rate for target capture and washing steps, enabling a short processing time of 1 min for 1 mL samples.

On-Chip RNP Denaturation, RT-PCR, and ssDNA Generation. Genetic detection from extremely low concentrations of captured viral RNA targets requires nucleic acid amplification (Figure 1D–G). In order to perform the amplification, we used a thermostable reverse transcriptase to thermally denature the RNP, releasing target RNA for concurrent reverse transcription to produce a cDNA template for subsequent PCR. In contrast to linear asymmetric PCR amplification for generation of ssDNA,[22,25,48] MIMED achieves higher ssDNA concentration via exponential PCR amplification and subsequent enzymatic dsDNA digestion. The dsDNA PCR amplicons were converted to ssDNA on chip by selective digestion of 5′-phosphorylated strands with lambda exonuclease[49] at high purity and efficiency (>90%). On-chip RT-PCR and ssDNA generation reactions proved reproducible, with efficiencies comparable to benchtop controls, and required no additional reagents or intermediate purification steps (Figure S3A). Furthermore, we observed only less than 5% reduction in sample volume during thermocycling in the device. In order to achieve the high efficiency, we designed the internal surface area of MIMED device to consist mostly of glass. Only ~6% of the internal surface area is PDMS, which is known to cause enzyme adsorption and significant sample loss at elevated temperatures.[36] Furthermore, we avoided the use of exposed ferromagnetic structures in the chamber, as they have been reported to nonspecifcally adsorb proteins.[39]

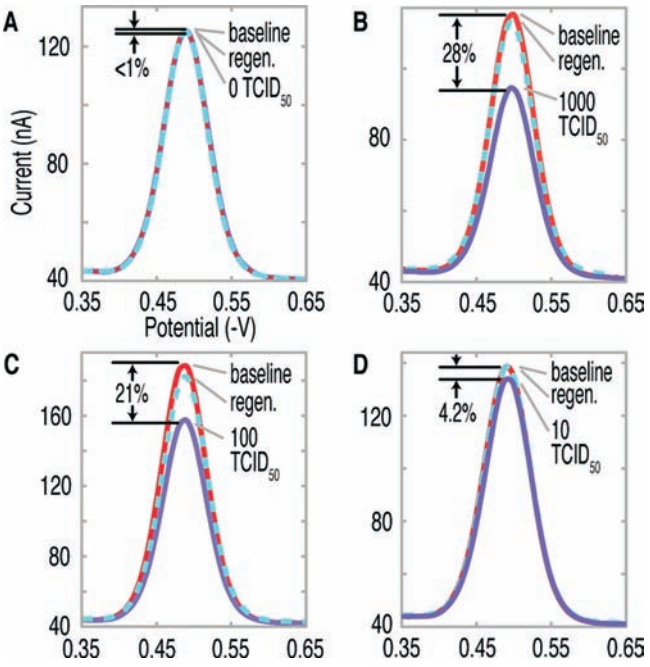

Figure 4. Limit of detection of MIMED is ~10 $TCID_{50}$. Swab samples containing 1000, 100, and 10 $TCID_{50}$ returned peak faradic current changes of 28, 21, and 4.2%, respectively, relative to 0.5% for negative control. All sensors could be regenerated to baseline levels, verifying that signal was the result of target hybridization.

E-DNA Sensor Characterization. E-DNA signaling is highly specific due to target binding-induced changes in the dynamics of the probe DNA and the relative scarcity of electroactive contaminants in the interrogation potential range.[37,38] Therefore, it offers direct detection of amplified ssDNA target in the PCR mixture without any intermediate separation or purification steps. For samples containing H1N1 virus ranging from 10 to 1000 $TCID_{50}$, typical amplified ssDNA concentrations range from 10 to 300 nM. To determine the time necessary to resolve this concentration range via E-DNA detection, we challenged the sensor with synthetic 62-base ssDNA target identical to the H1N1 amplicon. We incubated the DNA targets at different concentrations in the electrochemical cell in high-salt buffer and collected square wave voltammograms (SWV) at 30 s intervals (Figure S3B). As expected, E-DNA responses were logarithmic with regard to concentration and approximately linear over time (for t < 10 min). Importantly, 10 nM ssDNA could be resolved within 30 min, indicating potential to detect 10 $TCID_{50}$ viral samples.

MIMED Performance in Throat Swab Samples. Complete MIMED assays were conducted directly with throat swab samples containing a range of H1N1 viral concentrations (Figure 4). As a negative control, we used samples without spiked virus. This produced <1% change in the E-DNA signal (Figure 4A), indicating the absence of specific amplification product and the complete lack of viral particles in the sample. Conversely, we obtained sensor signals of 28%, 21%, and 4.2% from samples respectively spiked with H1N1 virus at 1000, 100, or 10 $TCID_{50}$, indicating the presence of specific product, corresponding to the range of initial viral content (Figure 4B, C). This result confirms the capacity of MIMED to achieve

unambiguous detection at concentrations as low as 10 $TCID_{50}$. This performance is reproducible; triplicate independent measurements performed with separate samples on separate devices yielded average signals of 31 ± 5.2%, 16 ± 4.2%, 3.0 ± 1.5%, and 0.91 ± 0.47% for samples containing H1N1 viruses at 1000, 100, 10, and 0 $TCID_{50}$, respectively. Importantly, the MIMED system directly offers a detection limit significantly below clinical titers of ~10^5 $TCID_{50}$ for throat swab samples[9] and a sensitivity improvement greater than 2 orders of magnitude over recently published values for rapid antigen tests against swine-origin influenza virus.[50]

CONCLUSION

We demonstrate an integrated microfluidic system, which enables sequence-specific viral RNA-based pathogen detection with high sensitivity and specificity from unprocessed throat swab samples. Using H1N1 influenza virus as a model, we have obtained a LOD of ~10 $TCID_{50}$ from throat swab samples directly, which is 4 orders of magnitude below clinically relevant viral titers, and more than two orders below rapid tests for swine-origin influenza virus. This performance was achieved by integrating immunomagnetic target capture, concentration and purification, RT-PCR amplification, and sequence-specific electrochemical detection in a single monolithic disposable device. The MIMED device is designed as an inexpensive disposable unit, which interfaces with an instrument containing supporting peripherals such as pumps and heaters. The sample preparation uses a simple microchamber without chemical or physical modifications, enabling high-throughput sample capture, minimal enzyme adsorption, favorable downstream enzymatic reactions, and high PCR efficiency. Total assay time is ~3.5 h, and the RT-PCR represents a rate-limiting step (~150 min). We believe further assay optimization and rapid thermal cycling strategies[51] may significantly reduce the assay time. Currently, the MIMED system is tuned for highest sensitivity;[52] however, for applications where large dynamic range is required, our system can be readily operated in parallel, for example, with undiluted sample for detecting lower titers and diluted sample for higher titers. Importantly, given the availability of affinity reagents for a broad range of pathogenic targets,[53] we believe our MIMED system represents a universal strategy toward multiplexed genetic detection of biological sample at the point-of-care.[54]

ASSOCIATED CONTENT

Supporting Information. Characterization data and experimental and fabrication details. This material is available free of charge via the Internet at http://pubs.acs.org.

AUTHOR INFORMATION

Corresponding Author
tsoh@engr.ucsb.edu

ACKNOWLEDGMENT

We are grateful for financial support from the Institute of Collaborative Biotechnologies through the Army Research Office, and the National Institutes of Health. We thank Jonathan Adams, Adriana Patterson, and Ryan White for valuable discussions, the Plaxco Lab for assistance in electrode preparation, and the UCSB Nanofabrication Facility.

REFERENCES

(1) Horsman, K. M.; Bienvenue, J. M.; Blasier, K. R.; Landers, J. P. *J. Forensic Sci.* **2007**, *52*, 784.
(2) Palchetti, I.; Mascini, M. *Anal. Bioanal. Chem.* **2008**, *391*, 455.
(3) Gardeniers, J. G. E.; van den Berg, A. *Anal. Bioanal. Chem.* **2004**, *378*, 1700.
(4) Holland, C. a.; Kiechle, F. L. *Curr. Opin. Microbiol.* **2005**, *8*, 504.
(5) Yang, S.; Rothman, R. *Lancet Infect. Dis.* **2004**, *4*, 337.
(6) Kling, J. *Nat. Biotechnol.* **2006**, *24*, 891.
(7) Bissonnette, L.; Bergeron, M. G. *Clin. Microbiol. Infect.* **2010**, *16*, 1044.
(8) Wilson, I. G. *Appl. Environ. Microbiol.* **1997**, *63*, 3741.
(9) Fouchier, R. A. M.; Bestebroer, T. M.; Herfst, S.; Van der Kemp, L.; Rimmelzwaan, G. F.; Osterhaus, A. D. M. E. *J. Clin. Microbiol.* **2000**, *38*, 4096.
(10) Spackman, E.; Suarez, D. L. *Methods Mol. Biol.* **2008**, *436*, 13.
(11) Andreoletti, L.; Hober, D.; Belaich, S.; Lobert, P. E.; Dewilde, A.; Wattre, P. *J. Virol. Methods* **1996**, *62*, 1.
(12) Hartshorn, K. L.; Ligtenberg, A.; White, M. R.; van Eijk, M.; Hartshorn, M.; Pemberton, L.; Holmskov, U.; Crouch, E. *Biochem. J.* **2006**, *393*, 545.
(13) Karch, H.; JanetzkiMittmann, C.; Aleksic, S.; Datz, M. *J. Clin. Microbiol.* **1996**, *34*, 516.
(14) Holland, J. L.; Louie, L.; Simor, A. E.; Louie, M. *J. Clin. Microbiol.* **2000**, *38*, 4108.
(15) Lou, Q.; Chong, S. K.; Fitzgerald, J. F.; Siders, J. A.; Allen, S. D.; Lee, C. H. *J. Clin. Microbiol.* **1997**, *35*, 281.
(16) Yager, P.; Edwards, T.; Fu, E.; Helton, K.; Nelson, K.; Tam, M. R.; Weigl, B. H. *Nature* **2006**, *442*, 412.
(17) Myers, F. B.; Lee, L. P. *Lab Chip* **2008**, *8*, 2015.
(18) Chen, L.; Manz, A.; Day, P. J. R. *Lab Chip* **2007**, *7*, 1413.
(19) Easley, C. J.; Karlinsey, J. M.; Bienvenue, J. M.; Legendre, L. a.; Roper, M. G.; Feldman, S. H.; Hughes, M. a.; Hewlett, E. L.; Merkel, T. J.; Ferrance, J. P.; Landers, J. P. *Proc. Natl. Acad. Sci. U.S.A.* **2006**, *103*, 19272.
(20) Zhang, C. S.; Xing, D. *Nucleic Acids Res.* **2007**, *35*, 4223.
(21) Kaigala, G. V.; Huskins, R. J.; Preiksaitis, J.; Pang, X.-L.; Pilarski, L. M.; Backhouse, C. J. *Electrophoresis* **2006**, *27*, 3753.
(22) Yeung, S. W.; Lee, T. M. H.; Cai, H.; Hsing, I. M. *Nucleic Acids Res.* **2006**, *34*, e118.
(23) Wang, J. *Biosens. Bioelectron.* **2006**, *21*, 1887.
(24) Drummond, T. G.; Hill, M. G.; Barton, J. K. *Nat. Biotechnol.* **2003**, *21*, 1192.
(25) Liu, R. H.; Yang, J. N.; Lenigk, R.; Bonanno, J.; Grodzinski, P. *Anal. Chem.* **2004**, *76*, 1824.
(26) Flint, S. J.; Racaniello, V. R.; Enquist, L.; Skalka, W. A. M. *Principles of Virology: Molecular Biology, Pathogenesis, and Control of Animal Viruses*, 2nd ed.; ASM Press: Herndon, VA, 2003.
(27) Kawakami, K.; Ishihama, A. *J. Biochem. (Tokyo, Jpn.)* **1983**, *93*, 989.
(28) Miltenyi, S.; Muller, W.; Weichel, W.; Radbruch, A. *Cytometry* **1990**, *11*, 231.
(29) Palecek, E.; Fojta, M. *Talanta* **2007**, *74*, 276.
(30) Adams, J. D.; Kim, U.; Soh, H. T. *Proc. Natl. Acad. Sci. U.S.A.* **2008**, *105*, 18165.
(31) Csordas, A.; Gerdon, A. E.; Adams, J. D.; Qian, J. R.; Oh, S. S.; Xiao, Y.; Soh, H. T. *Angew. Chem., Int. Ed.* **2010**, *49*, 355.
(32) Qian, J. R.; Lou, X. H.; Zhang, Y. T.; Xiao, Y.; Soh, H. T. *Anal. Chem.* **2009**, *81*, 5490.
(33) Pamme, N. *Lab Chip* **2006**, *6*, 24.
(34) Fonnum, G.; Johansson, C.; Molteberg, A.; Morup, S.; Aksnes, E. *J. Magn. Magn. Mater.* **2005**, *293*, 41.
(35) Kim, J. A.; Lee, J. Y.; Seong, S.; Cha, S. H.; Lee, S. H.; Kim, J. J.; Park, T. H. *Biochem. Eng. J.* **2006**, *29*, 91.
(36) Shin, Y. S.; Cho, K.; Lim, S. H.; Chung, S.; Park, S. J.; Chung, C.; Han, D. C.; Chang, J. K. *J. Micromech. Microeng.* **2003**, *13*, 768.
(37) Fan, C. H.; Plaxco, K. W.; Heeger, A. J. *Proc. Natl. Acad. Sci. U.S.A.* **2003**, *100*, 9134.

(38) Xiao, Y.; Lubin, A. A.; Heeger, A. J.; Plaxco, K. W. *Angew. Chem., Int. Ed.* **2005**, *44*, 5456.
(39) Williams, D. F.; Askill, I. N.; Smith, R. *J. Biomed. Mater. Res.* **1985**, *19*, 313.
(40) Reske, T.; Mix, M.; Bahl, H.; Flechsig, G. U. *Talanta* **2007**, *74*, 393.
(41) Little, J. W. *J. Biol. Chem.* **1967**, *242*, 679.
(42) Chomczynski, P.; Sacchi, N. *Anal. Biochem.* **1987**, *162*, 156.
(43) Bernard, P. S.; Wittwer, C. T. *Clin. Chem.* **2002**, *48*, 1178.
(44) Krafft, A. E.; Russell, K. L.; Hawksworth, A. W.; McCall, S.; Irvine, M.; Daum, L. T.; Connoly, J. L.; Reid, A. H.; Gaydos, J. C.; Taubenberger, J. K. *J. Clin. Microbiol.* **2005**, *43*, 1768.
(45) Kumar, S. V.; Hurteau, G. J.; Spivack, S. D. *Clin. Cancer Res.* **2006**, *12*, 5033.
(46) Spackman, E.; Senne, D. A.; Myers, T. J.; Bulaga, L. L.; Garber, L. P.; Perdue, M. L.; Lohman, K.; Daum, L. T.; Suarez, D. L. *J. Clin. Microbiol.* **2002**, *40*, 3256.
(47) Liu, Y. L.; Adams, J. D.; Turner, K.; Cochran, F. V.; Gambhir, S. S.; Soh, H. T. *Lab Chip* **2009**, *9*, 3604.
(48) Lee, T. M. H.; Carles, M. C.; Hsing, I. M. *Lab Chip* **2003**, *3*, 100.
(49) Ferguson, B. S.; Buchsbaum, S. F.; Swensen, J. S.; Hsieh, K.; Lou, X. H.; Soh, H. T. *Anal. Chem.* **2009**, *81*, 6503.
(50) Chan, K. H.; Lai, S. T.; Poon, L. L. M.; Guan, Y.; Yuen, K. Y.; Peiris, J. S. M. *J Clin. Virol.* **2009**, *45*, 205.
(51) Zhang, C. S.; Xing, D. *Nucleic Acids Res.* **2007**, *35*, 4223.
(52) Petric, M.; Comanor, L.; Petti, C. A. *J. Infect. Dis.* **2006**, *194*, S98.
(53) Olsvik, O.; Popovic, T.; Skjerve, E.; Cudjoe, K. S.; Hornes, E.; Ugelstad, J.; Uhlen, M. *Clin. Microbiol. Rev.* **1994**, *7*, 43.
(54) Pavlovic, E.; Lai, R. Y.; Wu, T. T.; Ferguson, B. S.; Sun, R.; Plaxco, K. W.; Soh, H. T. *Langmuir* **2008**, *24*, 1102.